

# Temperature-memory polymer actuators

Marc Behl, Karl Kratz, Ulrich Noechel, Tilman Sauter, and Andreas Lendlein<sup>1</sup>

Institute of Biomaterial Science and Berlin-Brandenburg Centre for Regenerative Therapies, Helmholtz-Zentrum Geesthacht, 14513 Teltow, Germany

Edited by Alexander M. Klibanov, Massachusetts Institute of Technology, Cambridge, MA, and approved June 12, 2013 (received for review January 30, 2013)

Reading out the temperature-memory of polymers, which is their ability to remember the temperature where they were deformed recently, is thus far unavoidably linked to erasing this memory effect. Here temperature-memory polymer actuators (TMPAs) based on cross-linked copolymer networks exhibiting a broad melting temperature range ( $\Delta T_m$ ) are presented, which are capable of a long-term temperature-memory enabling more than 250 cyclic thermally controlled actuations with almost constant performance. The characteristic actuation temperatures  $T_{act}$ s of TMPAs can be adjusted by a purely physical process, guiding a directed crystallization in a temperature range of up to 40 °C by variation of the parameter  $T_{sep}$  in a nearly linear correlation. The temperature  $T_{sep}$  divides  $\Delta T_m$  into an upper  $T_m$  range ( $T > T_{sep}$ ) forming a reshapeable actuation geometry that determines the skeleton and a lower  $T_m$  range ( $T < T_{sep}$ ) that enables the temperature-controlled bidirectional actuation by crystallization-induced elongation and melting-induced contraction. The macroscopic bidirectional shape changes in TMPAs could be correlated with changes in the nanostructure of the crystallizable domains as a result of in situ X-ray investigations. Potential applications of TMPAs include heat engines with adjustable rotation rate and active building facades with self-regulating sun protectors.

reversible shape-memory polymer | active movement

The alignment and coupling of thermally controlled volume changes on the nanoscale has emerged as most important working principle to translate shape changes from the nanolevel to the macrolevel in polymers (1–4). In stimuli-responsive polymers capable of a free-standing shape-changing effect, this alignment is achieved during synthesis or processing by either application of external stress or the utilization of templates and fixed by covalent cross-links (5–12). Once synthesis is completed, the geometry of the shape change cannot be changed anymore (13–15) and the actuation temperature is fixed; this relies on thermal transitions with a defined temperature. Here we explored whether it is possible to implement a thermally controlled bidirectional actuation into free-standing polymers by purely physical manipulation enabling to adjust (repeatedly) the actuation temperature and (shape changing) geometry.

Although programmable shape changes have been realized in shape-memory polymers (SMPs), this effect is generally a one-time, one-way effect in free-standing SMPs (16–18). In SMPs the switching domains, which can solidify by crystallization or vitrification, provide two functions: they determine the geometry of the shape change and cause the entropy elastic recovery. A reversible movement could be observed when polymers with crystallizable segments are held under an externally applied constant stress (3, 8). Recently temperature-memory polymers (TMPs) enabled the programming of the switching temperature (19, 20). Also this temperature-memory effect (TME) is limited to a one-time, one-way effect. The aim of the current work was to develop polymers capable of a sustainable TME, which can perform a large number of reversible actuation cycles upon cooling and heating.

We hypothesized that a temperature-memory polymer actuator with programmable actuation temperature and (shape changing) geometry requires a reshapeable internal skeleton to implement or adjust the alignment of nanoscaled actuation domains. This demands anchor points, which enable the orientation

of the internal skeleton. The skeleton must be, on the one hand, capable of maintaining the alignment over several heating and cooling cycles and, on the other hand, sufficiently elastic in order to enable shape changes. The stress originating or caused by the coupled nanoscaled volume changes must be well balanced with the entropy elastic recovery stress, which is largely influenced by the skeleton-forming domains. Therefore, a sufficiently elastic component needs to be incorporated. Lastly, actuation domains with programmable actuation temperature need to be implemented.

Based on these assumptions, we derived a structural model for such programmable actuators (Fig. 1A). It is comprised of an internal skeleton formed by crystallites, which cluster on the nanoscale into a physical network comparable to a framework formed by brick bonds and actuation domains aligned in the frames. Upon cooling, the actuation domains expand in the direction of alignment. Hereby the frame is extended via increasing the interbrick distance. The macroscopic form stability of the skeleton after contraction of the actuation domains upon heating is given by the horizontal displacement of the bricks in the bond. Although the feasibility of this concept of actuators spanned in a framework of brick bonds could be recently demonstrated in a copolymer network, in which the framework and the actuator elements were provided by two chemically different polymer segments (21); the challenge for a temperature-memory actuator is the adjustment of the actuation temperature by a physical parameter, which should be enabled in addition to a programmable actuation geometry.

Our concept for implementing a temperature-memory in bidirectional actuators is a polymer network system, in which skeleton-forming and actuation domains are interchangeable. This is given if they are chemically identical. In such polymer networks, both domains types as well as their mechanical interplay can be adjusted by solely varying a physical parameter.

Crystallites were selected as nanoscaled structural elements, as they can act as bricks as well as thermally controlled volume-changing units. A semicrystalline polymer network providing a broad  $T_m$  range spanning from  $T_{m,onset}$  to  $T_{m,offset}$  associated to one polymer chain segment type allows the subdivision of the crystallites in two groups according to their associated  $T_m$ . Crystallites associated with the lower  $T_m$  range from  $T_{m,onset} \sim T_{low}$  to a temperature ( $T_{sep}$ ) (Fig. 1B, *Top*), which separates the lower and the upper  $T_m$  range, provide the actuation function. Crystallites of the upper  $T_m$  range from  $T_{sep}$  to  $T_{m,offset} \sim T_{prog}$  are used as crystallizable skeleton-forming domains. In this way, the weight ratio of the crystallites in the actuation and in the skeleton-forming domains can be adjusted by the variation of  $T_{sep}$ . Repetitively changing the temperature between  $T_{low}$  and  $T_{sep}$  results in subsequent melting and recrystallization of the actuation domains (Fig. 1B, *Middle*).

Author contributions: M.B., K.K., and A.L. designed research; M.B., K.K., U.N., and T.S. performed research; M.B., K.K., U.N., T.S., and A.L. analyzed data; and M.B., K.K., and A.L. wrote the paper.

The authors declare no conflict of interest.

This article is a PNAS Direct Submission.

Freely available online through the PNAS open access option.

<sup>1</sup>To whom correspondence should be addressed. E-mail: andreas.lendlein@hzg.de.

This article contains supporting information online at [www.pnas.org/lookup/suppl/doi:10.1073/pnas.1301895110/-DCSupplemental](http://www.pnas.org/lookup/suppl/doi:10.1073/pnas.1301895110/-DCSupplemental).

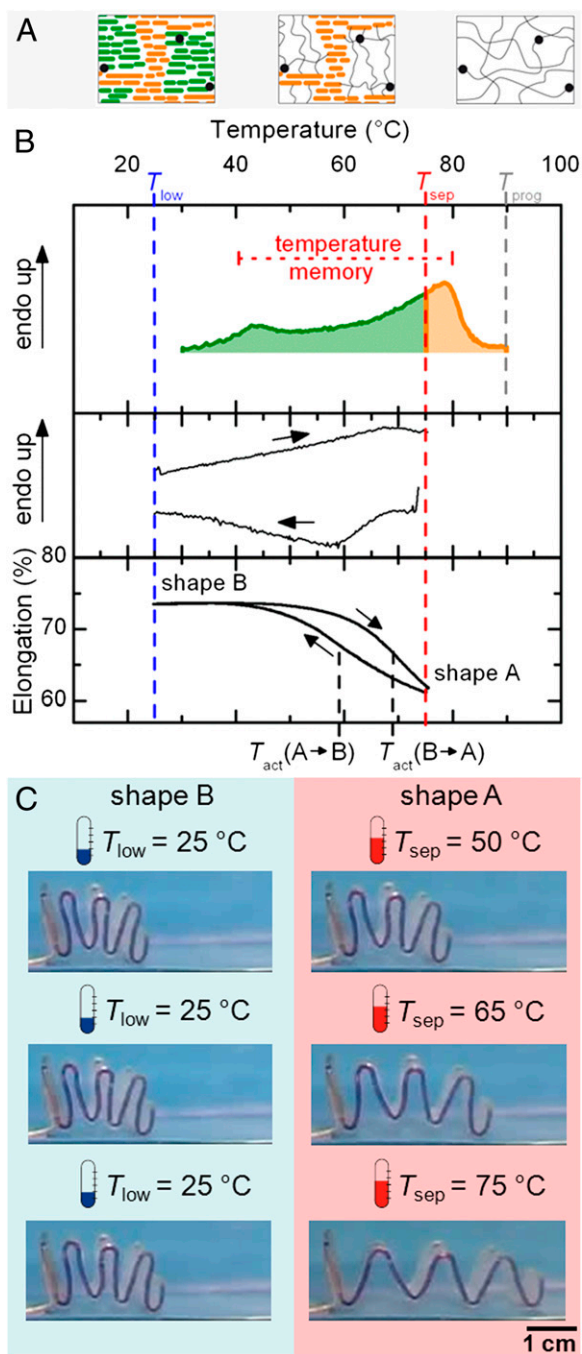


**Fig. 1.** Working principle of the programmable temperature-memory polymer actuator. (A) Programming: Amorphous sample is deformed at  $T_{prog}$  (Right); ● chemical cross-links. At  $T_{sep}$  (Center) appearance is determined by the directed crystallization of the internal skeleton-forming domains (red). Actuation: reversible shape changes are realized in the polymer by crystallization/melting of oriented polyethylene segments in the actuation domains (green) between  $T_{low}$  and  $T_{sep}$  (Left). (B) Thermal and thermo-mechanical investigations of cPEVA. DSC apparatus specific transient signal oscillation at the beginning and at the end of temperature ramps not shown. (Top) The  $T_{sep}$  divides crystallizable domains in geometry determining and actuation domains. (Middle) Thermogram of first actuation cycle. A melting peak with a peak maximum, which is significantly lower compared with the peak maximum obtained when the sample was completely molten (Top), can be observed. (Bottom) Elongation as function of temperature, first reversible actuation cycle for  $T_{prog} = 90^\circ\text{C}$ ,  $\epsilon_{ssp} = 150\%$ ,  $T_{low} = 25^\circ\text{C}$ ,  $T_{sep} = 75^\circ\text{C}$  (shapes A, B, black line). Shape A is obtained as  $\epsilon_A$  at  $T_{sep}$ . Cooling to  $T_{low}$  results in shape B corresponding to  $\epsilon_B$ . Heating to  $T_{sep}$  recovers  $\epsilon_A$  again. (C) Photo series illustrating the temperature-memory

The anisotropic volume changes of the actuation domains are based on conformational orientation of chain segments during crystallization (elongation) or recoiling after melting (contraction), which only occurs if these domains are aligned within the skeleton and coupled by the covalent net points as anchor points of the polymer networks. In this way the effects on the molecular level are translated to macroscopic shape changes. Therefore, the skeleton formed by the crystallites  $> T_{sep}$  must be built in such a way that the chains within the actuation domains are oriented in the direction of the targeted macroscopic shape shift. For this purpose a macroscopic deformation ( $\epsilon_{ssp}$ ) according to the desired appearance is required at  $T_{prog}$ . The skeleton is formed by cooling under stress to  $T_{low}$ , at which the chain segments crystallize. Shape A is achieved after heating to  $T_{sep}$  under stress-free condition (Fig. 1B, Bottom) and now implemented in the material. We name this process to define the actuation temperature and to alter the appearance programming. Cooling to  $T_{low}$  results in shape B. Reheating to  $T_{sep}$  causes melting of the actuation domains and results in shape A again. The changes in dimension, which are directed oppositely to the thermal expansion during heating and shrinkage upon cooling, occur at maximum velocity at the actuation temperatures  $T_{act}(A \rightarrow B)$  and  $T_{act}(B \rightarrow A)$ .

## Results and Discussion

For designing a TMPA based on the aforementioned concept, a suitable polymer material requires a single broad melting transition for achieving a temperature-memory capability and the separation into skeleton-forming and actuation domains, a sufficient elasticity enabling the reversible deformation of the skeleton during actuation, and covalent net points for transferring the applied macroscopic deformation to the skeleton-forming and actuation domains.

As material basis we selected covalently cross-linked poly [ethylene-*co*-(vinyl acetate)] (cPEVA) (22–24) comprising crystallizable polyethylene (PE) segments. The repeating units of vinyl acetate contribute to a broad melting transition of PE crystallites spanning over a temperature interval from around  $25^\circ\text{C}$  to around  $90^\circ\text{C}$ . In addition, the related amorphous phase contributes to the elastic deformability of the skeleton. The covalent cross-links provide form stability at  $T_{prog}$  for elongation to  $\epsilon_{ssp}$  during programming and in this way allow the orientation of both actuator and skeleton-forming PE domains.

In Fig. 1C the temperature-memory actuation of cPEVA20d20 containing 20 wt% of vinyl acetate repeating units, which was cross-linked by 2 wt% of thermosensitive dicumyl peroxide in the starting material mixture (for details see *Materials and Methods*), is shown. A ribbon, which was programmed at  $T_{prog} = 90^\circ\text{C}$ , changes between an expanded concertina (shape A) and a contracted concertina (shape B) at constant  $T_{low}$  (Movie S1). Here,  $T_{act}$  of the programmed ribbon could be systematically adjusted by solely varying  $T_{sep}$ . This capability of TMPA elements might be used in building facades capable of controlling the degree of darkening according to the temperature (see Fig. 4A).

The actuation geometry of cPEVA is reprogrammable (Movie S2). Heating to  $T_{prog} = 90^\circ\text{C}$  erases the internal skeleton and new actuation geometries (butterfly or fastener device) can be programmed. During cyclic heating to  $75^\circ\text{C}$  and cooling to  $25^\circ\text{C}$ , shape changes occurred at the same  $T_{act}$ s as defined by  $T_{sep}$  independent from the appearance.

actuation capability of a cPEVA ribbon ( $80 \times 20 \times 0.9$  mm), which was inked at its edges with blue color to enhance contrast. A concertina appearance was created by folding at  $T_{prog} = 90^\circ\text{C}$ , cooling to  $T_{low} = 25^\circ\text{C}$ , and heating to  $T_{sep}$ , which was varied. The concertina shifted reversibly between an expanded concertina (shape A) and a contracted concertina (shape B).



actuator as it did not show any change in performance after 120 cycles programmed at  $\varepsilon_{ssp} = 100\%$  followed by additional 130 cycles after reprogramming with  $\varepsilon_{ssp} = 150\%$  (Fig. 2C).

The crystallizable domains are mandatory to achieve a temperature-memory actuation in polymer materials. Cross-linked polystyrene (cPS) (*SI Materials and Methods, Methods 1*) with a cross-linking density similar to cPEVA20d20 and a  $T_g = 95^\circ\text{C}$  was investigated in thermomechanical tests (with  $T_{prog} = 105^\circ\text{C}$ ;  $T_{sep} = 85^\circ\text{C}$ ,  $90^\circ\text{C}$ ,  $95^\circ\text{C}$ ,  $100^\circ\text{C}$ ;  $T_{low} = 25^\circ\text{C}$ ; and  $\varepsilon_{ssp} = 100\%$ ). Here, cPS did not show any actuation capability, only thermal expansion upon heating was observed. However, a certain weight content of amorphous domains is essential for gaining a bidirectional actuation, which was created by incorporation of a comonomer such as vinyl acetate. The cross-linked homopolymer low-density polyethylene did not show a temperature-memory actuator capability (Table S1). For all investigated cPEVAs comprising a vinyl acetate content in the range of 10–35 wt%, a pronounced temperature-memory actuation capability for  $T_{sep}$  between  $40^\circ\text{C}$  and  $90^\circ\text{C}$  (Table S1) was observed whereby the temperature interval for variation of  $T_{sep}$  was found to decrease with increasing comonomer content. The covalent cross-links are necessary for a TMPA. The linear copolymer PEVA did not show a bidirectional actuation. The applied macroscopic deformation during programming did not result in the required orientation of actuation domains because of the missing covalent net points interlinking the actuation and the skeleton-forming domains.

In situ wide-angle X-ray scattering (WAXS) and small-angle X-ray scattering (SAXS) measurements were performed to explore structural changes on the nanoscale for cPEVA20d20 during thermally controlled actuation (Fig. 3). At  $T_{sep}$  the achieved anisotropic scattering pattern can be attributed solely to the crystalline, skeleton PE domains, whose orientations become apparent in the anisotropic WAXS diffraction patterns (Fig. 3A). The achieved SAXS data revealed that the lamellae were oriented orthogonally to the direction of the macroscopic deformation (Fig. 3B). Here at  $T_{sep}$  a long-period  $L(T_{sep}) = 15.4$  nm was determined for a cPEVA programmed with  $\varepsilon_{ssp} = 150\%$ ; whereas, at  $T_{low}$  a long-period  $L(T_{low}) = 11.4$  nm was obtained. After reprogramming with  $\varepsilon_{ssp} = 100\%$ , the sample exhibited a  $L(T_{sep}) = 16.1$  nm and  $L(T_{low}) = 13.1$  nm. According to our hypothesis, the macroscopic change during actuation should be reflected on the nanoscale by changes of the long period. Based on the experimentally determined data at  $T_{sep}$  ( $\varepsilon_{ssp} = 150\%$ ) and the macroscopic changes in length and crystallinity during cooling

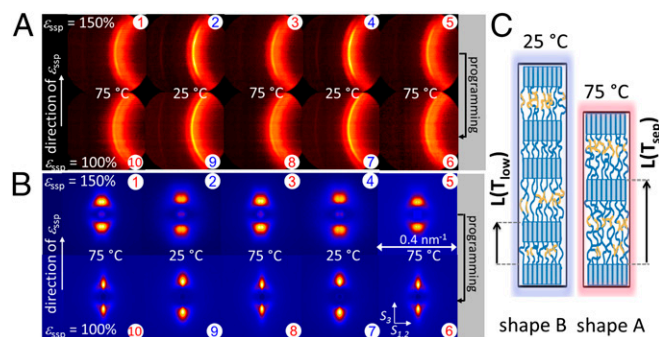


**Fig. 3.** Structural changes occurring during the bidirectional actuation of a programmed cPEVA20d20 ribbon. (A and B) Changes of the scattering pattern determined by 2D WAXS (A) and 2D SAXS (B) recorded for shapes A and B as well as for shapes A' and B' after (re)programming and in subsequent reversible actuation cycles. ( $T_{sep} = 75^\circ\text{C}$ ,  $T_{low} = 25^\circ\text{C}$ , upper series  $\varepsilon_{ssp} = 150\%$ , and lower series  $\varepsilon_{ssp} = 100\%$ ). Numbers indicate steps during experiment. (C) Changes of long periods schematically shown for cPEVA during bidirectional actuation.

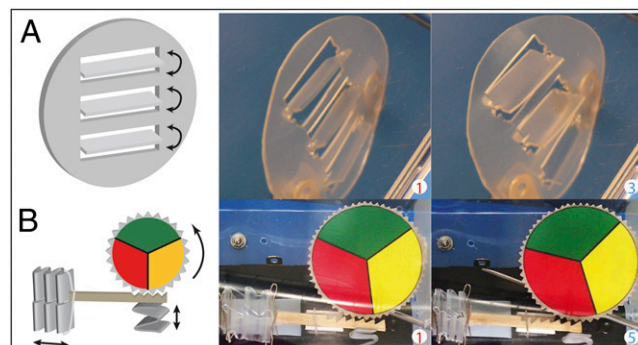


**Fig. 4.** Demonstration of the programmable actuation capability of cPEVA. Parameters of experiment:  $T_{prog} = 90^\circ\text{C}$ ,  $T_{sep} = 75^\circ\text{C}$ ,  $T_{low} = 25^\circ\text{C}$ . (A) (Left) Schematic illustration of the related shape change in a cPEVA based demonstrator providing programmable window shades. (Right) After programming the window shades to close upon heating and open when cooled. (B) Heat engine driven by a concertina-shaped cPEVA drive element, which moves an attached toothed rack forward when heated to  $T_{sep}$  and back when cooled to  $T_{low}$ , whereby its contact pressure to the tooth wheel is controlled by a second cPEVA concertina. Upon cooling to  $T_{low}$ , this concertina contracts resulting in a lower pressure on the rack enabling the driving element to contract as well. The number of folds in the driving element determines the distance of the forward motion. In this way the rotation speed of the tooth wheel can be adjusted by the programming of the driving element. The numbers indicate the cycle number of the actuation cycles.

to  $T_{low}$  an estimated long period at  $T_{low}$  could be calculated to  $L(T_{low}) = 10.7$  nm (*SI Materials and Methods, Methods 2*), which corresponds well with the experimental results.

The generality of our concept for designing a temperature-memory polymer actuator was demonstrated by transferring this strategy to a different copolymer network cPCLBA, containing crystallizable poly( $\varepsilon$ -caprolactone) (PCL) segments (Fig. S2 and *SI Materials and Methods, Methods 1*). The PCL domains provide a  $\Delta T_m$  between  $5^\circ\text{C}$  and  $60^\circ\text{C}$ , which can be used for the skeleton-forming and actuation function while the amorphous poly( $n$ -butylacrylate) containing domains ensure the material's elasticity. In cyclic, thermomechanical tests with  $\varepsilon_{ssp} = 150\%$  at  $T_{prog} = 60^\circ\text{C}$  a pronounced temperature-memory actuation capability could be achieved for cPCLBA. By variation of  $T_{sep}$  between  $40^\circ\text{C}$  and  $50^\circ\text{C}$  the actuation temperatures could be adjusted in the range between  $22 \pm 1$  and  $43 \pm 1^\circ\text{C}$  (Fig. S2) and an  $\varepsilon'_{rev}$  up to 19% was determined. Furthermore the reversible shape change between a flat shape at  $T_{sep} = 43^\circ\text{C}$  and a concertina-like shape at  $T_{low} = 0^\circ\text{C}$  was shown.

It can be anticipated that temperature-memory polymer actuators with long-term stability over many cycles, whose actuation temperatures and appearance can be adjusted in a purely physical process, and which are based on commodity polymers (e.g., PEVA), build a cornerstone for innovation in various fields. Examples for potential applications, which are illustrated as demonstrators from cPEVA20d20 (Fig. 4) are heat engines with adjustable rotation rate (Movie S3) or thermally controlled facades providing a self-sufficiently controlled sun protection with adjustable application temperature range.

## Materials and Methods

**Materials.** The cPEVAs were prepared by mixing 98 g poly[ethylene-co-(vinyl acetate)] with a vinyl acetate content of 9 wt% (Greenflex ML30, Polimeri Europa, cPEVA10) or of 18 wt% (Elvax460, DuPont, cPEVA20) and 2 g dicumyl peroxide (Sigma-Aldrich) in a twin-screw extruder (EuroPrismLab, Thermo Fisher Scientific) at  $110^\circ\text{C}$  and 50 rpm. The blends were compression molded into films with 1 mm thickness and subsequently cross-linked at  $200^\circ\text{C}$  and 20 bar for 25 min (20).

**Methods.** Quantifications of the temperature-memory actuation capability were conducted by cyclic, thermomechanical tensile tests with a standardized sample shape (ISO 527-2/1BB) on a Zwick Z1.0 machine equipped with a thermo-chamber and a 200-N load cell. The experiment consisted of an initial skeleton-formation module (called programming) and subsequent reversible actuation cycles. In the programming module, the sample was stretched with a rate of  $5 \text{ mm} \cdot \text{min}^{-1}$  to  $\epsilon_{\text{ssp}}$  at  $T_{\text{prog}}$  and equilibrated for 5 min. After cooling to  $T_{\text{low}}$  under constant strain and 10 min equilibration time the sample was reheated to  $T_{\text{sep}}$  under stress-free conditions, resulting in shape A. The reversible actuation cycle consisted of cooling to  $T_{\text{low}}$ , waiting for 10 min and reheating to  $T_{\text{sep}}$  followed by another waiting period of 10 min. Heating and cooling rates were  $1 \text{ K} \cdot \text{min}^{-1}$ , in long-term experiment  $5 \text{ K} \cdot \text{min}^{-1}$ . In experiments in which  $T_{\text{sep}}$  was varied, the programming module and an actuation cycle starting with the lowest  $T_{\text{sep}}$  were conducted. Afterward  $T_{\text{sep}}$  was raised and, after a waiting period of 5 min, a subsequent actuation cycle was carried out.

WAXS measurements were performed using an X-ray diffraction system Bruker D8 Discover with a 2D Hi-Star detector ( $105\text{-}\mu\text{m}$  pixel size) from Bruker AXS. The X-ray generator was operated at a voltage of 40 kV and a current

of 40 mA on a copper anode. A graphite monochromator produced  $\text{Cu-K}\alpha$  radiation (0.154 nm wavelength) and a three-pinhole collimator with an opening of 0.8 mm was used. The distance between sample and detector was 150 mm, calibrated with Corundum standard. In situ measurements at fixed stages during programming were performed using a custom-build stretching device, a heating gun, and a cooled nitrogen gas stream at 5 min exposure time per scattering pattern.

SAXS was performed on a Bruker AXS Nanostar diffractometer using a 2D VANTEC-2000 detector. The distance sample to detector was 1,070 mm, the beamsize  $400 \mu\text{m}$ , and the wavelength 0.154 nm. The 2D-scattering patterns were integrated after background subtraction over a  $10^\circ$  wide chi range along the  $s_3$  axis (drawing direction) were discrete peaks were observed, leading into a one-dimensional curve  $I$  vs.  $s_3$ . Long periods were determined from the position of the peak maxima after Lorentz correction ( $I(s) \rightarrow s^2 I(s)$ ) as  $L = 1/s_L$ .

**ACKNOWLEDGMENTS.** The authors are grateful to Narendra Kumar for assistance with graphics and movies and Jing Cui for synthesis of cPCLBA. This work was financially supported by the Helmholtz Association.

- De Gennes PG (1975) One type of nematic polymers. *Roy Acad. Sci Ser B* 281(5-8): 101–103.
- Adams JM, Warner M, Stenull O, Lubensky TC (2008) Smectic-A elastomers with weak director anchoring. *Phys Rev E Stat Nonlin Soft Matter Phys* 78(1 Pt 1):011703.
- Chung T, Romo-Uribe A, Mather PT (2008) Two-way reversible shape memory in a semicrystalline network. *Macromolecules* 41(1):184–192.
- Zotzmann J, Behl M, Hofmann D, Lendlein A (2010) Reversible triple-shape effect of polymer networks containing polypentadecalactone- and poly( $\epsilon$ -caprolactone)-segments. *Adv Mater* 22(31):3424–3429.
- Stuart MAC, et al. (2010) Emerging applications of stimuli-responsive polymer materials. *Nat Mater* 9(2):101–113.
- van Oosten CL, Bastiaansen CWM, Broer DJ (2009) Printed artificial cilia from liquid-crystal network actuators modularly driven by light. *Nat Mater* 8(8):677–682.
- Zhang X, et al. (2011) Optically- and thermally-responsive programmable materials based on carbon nanotube-hydrogel polymer composites. *Nano Lett* 11(8):3239–3244.
- Mandelkern L, Roberts DE, Diorio AF, Posner AS (1959) Dimensional changes in systems of fibrous macromolecules - Polyethylene. *J Am Chem Soc* 81(16):4148–4157.
- Sánchez C, Verbakel F, Escuti MJ, Bastiaansen CWM, Broer DJ (2008) Printing of monolithic polymeric microstructures using reactive mesogens. *Adv Mater* 20(1): 74–78.
- Ohm C, Serra C, Zentel R (2009) A continuous flow synthesis of micrometer-sized actuators from liquid crystalline elastomers. *Adv Mater* 21(47):4859–4862.
- Hong SJ, Yu WR, Youk JH (2010) Two-way shape memory behavior of shape memory polyurethanes with a bias load. *Smart Mater Struct* 19(3):035022.
- Xu J, Song J (2010) High performance shape memory polymer networks based on rigid nanoparticle cores. *Proc Natl Acad Sci USA* 107(17):7652–7657.
- Ikedo T, Mamiya J, Yu YL (2007) Photomechanics of liquid-crystalline elastomers and other polymers. *Angew Chem Int Ed Engl* 46(4):506–528.
- Urayama K (2007) Selected issues in liquid crystal elastomers and gels. *Macromolecules* 40(7):2277–2288.
- Fleischmann E-K, et al. (2012) One-piece micropumps from liquid crystalline core-shell particles. *Nat Commun* 3:1178.
- Mather PT, Luo XF, Rousseau IA (2009) Shape memory polymer research. *Annu Rev Mater Res* 39:445–471.
- Huang WM, et al. (2010) Shape memory materials. *Mater Today* 13(7-8):44–51.
- Hu J, Zhu Y, Huang H, Lu J (2012) Recent advances in shape-memory polymers: Structure, mechanism, functionality, modeling and applications. *Prog Polym Sci* 37(12): 1720–1763.
- Xie T, Page KA, Eastman SA (2011) Strain-based temperature memory effect for n-fion and its molecular origins. *Adv Funct Mater* 21(11):2057–2066.
- Kratz K, Voigt U, Lendlein A (2012) Temperature-memory effect of copolyesterurethanes and their application potential in minimally invasive medical technologies. *Adv Funct Mater* 22(14):3057–3065.
- Behl M, Kratz K, Zotzmann J, Lendlein A (2013) Reversible Bidirectional Shape-memory Polymers. *Adv Mater*, 10.1002/adma.201300880.
- de Souza CMG, Tavares MIB (1998) NMR study of commercial poly(ethylene-co-vinyl acetate). *Polym Test* 17(8):533–541.
- Hobeika S, Men Y, Strobl G (2000) Temperature and strain rate independence of critical strains in polyethylene and poly(ethylene-co-vinyl acetate). *Macromolecules* 33(5):1827–1833.
- Kratz K, Madbouly SA, Wagermaier W, Lendlein A (2011) Temperature-memory polymer networks with crystallizable controlling units. *Adv Mater* 23(35):4058–4062.